Polymer Chemistry

Microstructure analysis of biocompatible phosphoester copolymers†

Tobias Steinbach,[abc] Romina Schröder,[a] Sandra Ritz[c] and Frederik R. Wurm[*c]

Copolymers with varying compositions of 2-ethoxy-2-oxo-1,3,2-dioxaphospholane (EEP) and 2-ethoxy-4-methyl-2-oxo-1,3,2-dioxaphospholane (EMEP) have been synthesized *via* 1,5,7-triazabicyclo[4.4.0]dec-5-ene-catalyzed anionic ring-opening polymerization. The molecular weights and comonomer ratios were well controlled and polymers with reasonable molecular weight distributions (<1.5) were obtained in all cases. The copolymers were investigated by ^{1}H and ^{31}P NMR spectroscopies to determine the underlying microstructure *via* detailed dyad analysis. The copolymers were found to be nontoxic to HeLa cells. Furthermore, the obtained copolymers of EEP and EMEP show thermoresponsive properties, *i.e.*, exhibit a lower critical solution temperature (LCST).

Introduction

Phosphorus-based polymers are a predominant class of materials in nature and are the source of life (DNA/RNA). In polymer science, however, they are scarcely investigated and only a few recent publications deal with much simpler polyphosphoesters (PPEs) in spite of their unique properties in bio-relevant, but also materials science applications.[1] On the other hand, poly-carboxylic esters are a typical example of synthetic polymers that are applied in biomedical applications due to their biocompatibility and degradability. However, when it comes to versatility, phosphoesters are in many cases superior to carboxylic acid esters due to the inherent capability of phosphates to form triesters, *i.e.* having a functional group at every repeating unit along the polymer backbone, but also as they possess three ester groups that can undergo hydrolysis. PPEs combine the excellent biocompatibility and biodegradability[2,3] (either by hydrolysis and/or by enzymatic degradation[4]) of conventional (carboxylic) polyesters, they are water-soluble in many cases and allow easy structural diversity with the chemical variability of the phosphorus center.
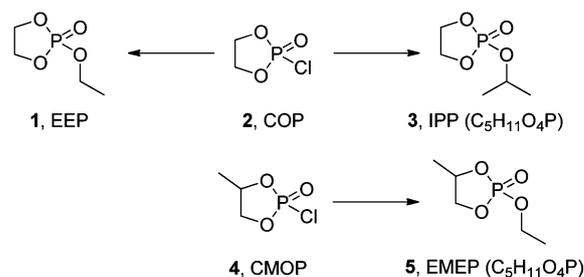
PPE chemistry was pioneered by Penczek and co-workers in the 1970s.[5–8] The biological potential of PPEs was immediately recognized since aliphatic PPEs resemble a simple model for essential biomacromolecules, deoxyribonucleic acid (DNA) and ribonucleic acid (RNA). First attempts to synthesize "artificial DNA" were also undertaken in Penczek's lab on the basis of poly(1,2-glycerol phosphate) prepared by ring-opening polymerization (ROP) of strained cyclic phosphoesters.[9–11]

Cyclic, five-membered or six-membered, phosphate monomers have been polymerized *via* cationic, anionic or enzymatic pathways. Recently, seven-membered unsaturated phosphates were polymerized *via* ring-opening metathesis polymerization.[12] Also acyclic diene metathesis polymerization was used to prepare PPEs.[13] Until the development of controlled polymerization techniques, such as the polymerization *via* stannous octoate (Sn(Oct)$_2$) or by aluminum *iso*-propoxide, well-defined structures and controlled molecular weights were difficult to achieve.[9,14,15]

ROP of phospholanes can also be catalyzed by organic bases, such as 1,8-diazabicyclo[5.4.0]-undec-7-ene (DBU) or 1,5,7-tri-azabicyclo[4.4.0]dec-5-ene (TBD). These bases allow excellent control over molecular weights and polydispersity avoiding metal catalysts providing a good basis for further biomedical applications.[16]

The structural versatility of PPEs was exploited by Iwasaki and co-workers to prepare novel thermoresponsive polymers

[a]*Institute of Organic Chemistry, Johannes Gutenberg-University (JGU), Duesbergweg 10-14, 55099 Mainz, Germany*

[b]*Graduate School Material Science in Mainz, Staudinger Weg 9, D-55128 Mainz, Germany*

[c]*Max Planck Institute for Polymer Research, Ackermannweg 10, 55128 Mainz, Germany. E-mail: wurm@mpip-mainz.mpg.de; Fax: +49 6131 370 330; Tel: +49 6131 379 723*

Scheme 1 Cyclic phosphate monomers synthesized from ethylene glycol (top) and EMEP synthesized from 1,2-propanediol (bottom). IPP and EMEP are isomers.

from 2-ethoxy-2-oxo-1,3,2-dioxaphospholane (EEP, **1**) and 2-isopropoxy-2-oxo-1,3,2-dioxaphospholane (IPP, **3**) (Scheme 1).[17] They observed a linear dependence of the cloud points on the copolymer composition. However, IPP is rather hydrophobic, so that copolymers consisting of more than 50 mol% IPP are not soluble in aqueous solutions above 20 °C.[17]

A typical way of tailoring the cloud point temperature of (co) polymers is the introduction of hydrophobic units into a hydrophilic polymer.[17–21] Based on this strategy we envisaged a comonomer derived from EEP that is not as hydrophobic as IPP, but its polymer still offers a lower critical solution temperature (LCST) in the physiological interesting region. Furthermore, the potential toxic effects of a degradation product, ethylene glycol (EG), needs to be addressed if any PPE prepared from 2-chloro-2-oxo-1,3,2-dioxaphospholane (COP, **2**) would be applied in the biomedical field. Both demands are fulfilled by the use of 1,2-propandiol instead of EG as the backbone-forming diol as it is approved as a food additive by the European Food Safety Authority and is "generally recognized as safe" by the US Food and Drug Administration. Additionally, 1,2-propandiol does not cause sensitization and no evidence of carcinogenic or genotoxic effects has been reported.[22] Propylene glycol is metabolized in the human body into pyruvic acid, acetic acid, lactic acid, and propionaldehyde.[23]

The first PPEs prepared from 1,2-propandiol were reported by Penczek and co-workers in 1982 based on the pioneering work of Zwierzak[24] and Nifant'ev[25] et al. who observed spontaneous polymerization of 4-methyl-2-oxo-2-hydro-1,3,2-dioxaphospholane. Penczek and co-workers established a route to synthesize racemic and optically active poly(4-methyl-2-oxo-2-hydro-1,3,2-dioxaphospholane) and the corresponding polyphosphoric acid by oxidation with dinitrogen tetroxide. This elaborate and demanding synthetic protocol is still employed by research groups interested in polyphosphates.[2,26,27]

Penczek was the first to investigate the detailed microstructure of the obtained poly(4-methyl-2-oxo-2-hydro-1,3,2-dioxaphospholane)s. Due to the limited NMR setup available (36.43 MHz for the phosphorus resonance), the authors were not able to observe the signal pattern a suitable dyad model predicted for the studied poly-H-phosphonates.[28] With the high resolution NMR equipment available today, a more elaborate analysis and a careful investigation of the underlying microstructure of phosphonate and phosphate polymers can be conducted. Furthermore, with organocatalysis many polyphosphates of interest can be synthesized in a highly controlled manner

avoiding side reactions which can interfere with the NMR data and its microstructure analysis.

First attempts to copolymerize 2-ethoxy-4-methyl-2-oxo-1,3,2-dioxaphospholane (EMEP, **5**) with 2-ethoxy-2-oxo-1,3,2-dioxaphospholane (EEP, **1**) initiated with triisobutylaluminum at different temperatures were reported by Brosse and coworkers in 1990.[29] However, no copolymerization was observed at ambient temperatures, but only the homopolymer of EEP was found. Only at elevated temperatures (90 °C) and for long reaction times (18 h) considerable copolymerization (comonomer incorporation between 50 and 90%) was observed with low yields (<50%). SEC analysis indicated a broad distribution of low molecular weights with a PDI around 2.5.

Derivatives of polypropylene phosphates are accessible via ring-opening polymerization of 4-methyl-2-oxo-2-hydro-1,3,2-dioxaphospholane followed by chlorination of the phosphite and esterification (with ethanol for example) of poly-(4-methyl-2-oxo-2-chloro-1,3,2-dioxaphospholane) to obtain poly-(4-methyl-2-oxo-2-ethyl-1,3,2-dioxaphospholane), PEMEP.[27] In this report, we have overcome this "H-phosphonate route" by preparing the monomer EMEP (**5**), analogously to the synthesis of EEP (**1**) as reported by Brosse and coworkers (Scheme 2).[30] Subsequent copolymerization reactions of the cyclic phosphoester monomers with TBD as the catalyst at 0 °C resulted in polyphosphates with narrow molecular weight distributions in less than 15 min polymerization time. The thermoresponsive properties of the polymers were investigated and the microstructure was analyzed by detailed NMR spectroscopic experiments for the first time. In addition, a series of viability tests on HeLa cells proved the high biocompatibility of the copolymers.

Experimental

Materials

Solvents were purchased from Acros Organics, Sigma Aldrich, or Fluka and used as received, unless otherwise stated.

Phosphorus trichloride was purchased from Sigma Aldrich. Ethanol, ethylene glycol and 1,2-propanediol were purchased from Sigma Aldrich and dried before use (distillation from sodium and stored over molecular sieves). All other chemicals were ordered from Sigma Aldrich and used as received.

Synthesis of monomers

2-Chloro-2-oxo-1,3,2-dioxaphospholane (COP, **2**) and 2-chloro-4-methyl-2-oxo-1,3,2-dioxaphospholane (CMOP, **4**) were synthesized
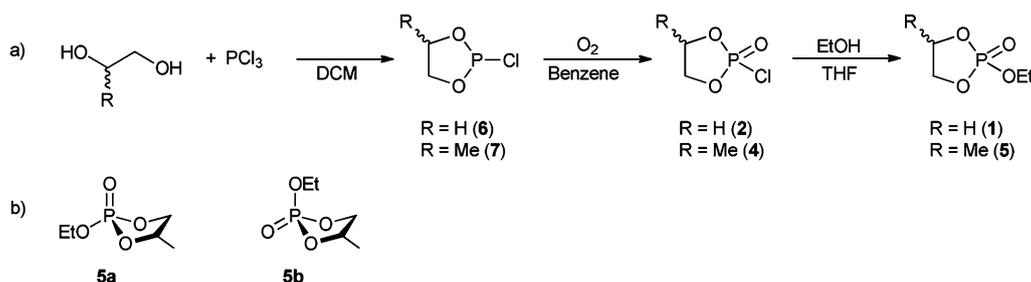
Scheme 2   (a) Synthesis of EEP (**1**) and EMEP (**5**). (b) The two possible conformers of EMEP (**5a** and **5b**) result in two distinct resonances in ^{31}P NMR spectroscopy.

by a modified literature protocol.[31] Briefly, a solution of 2-chloro-1,3,2-dioxaphospholane[32] (**6**, 98.15 g, 780 mmol) in benzene (500 mL) was heated to 50 °C. A stream of oxygen was passed through the solution. Unreacted oxygen was recovered by recycling the gas employing a peristaltic pump. The consumption of oxygen was monitored by the decrease in volume of the used reservoir balloon (scheme of the experimental setup in Fig S1, ESI†). Subsequently, the solvent was removed *in vacuo*. Distillation of the residue yielded COP (62.7 g, 57%, b.p. 95 °C/13 Pa) in high purity. ^{1}H NMR (CDCl$_3$): δ 4.69–4.38 (m, 4H, O–CH_2–CH_2–O).

2-Ethoxy-2-oxo-1,3,2-dioxaphospholane (1, EEP)

1 was synthesized by the esterification of 2-chloro-2-oxo-1,3,2-dioxaphospholane (**2**) with ethanol under an inert atmosphere. Briefly, a solution of dry ethanol (20.48 g, 450 mmol) and dry pyridine (35.50 g, 450 mmol) in dry THF (20 mL) was added dropwise to a stirred solution of 2-chloro-2-oxo-1,3,2-dioxaphospholane (61.7 g, 430 mmol) in dry THF (200 mL) at −21 °C within 45 min. Complete precipitation of pyridinium hydrochloride was achieved by storage at −21 °C overnight. After filtration the filtrate was concentrated *in vacuo*. The residue was distilled under reduced pressure to give the desired product (37.0 g, 56%, b.p. 93 °C/1.6 Pa). ^{1}H NMR (CDCl$_3$): δ 1.34 (t, 3H, –CH_3, ^3J 6.0 Hz), 4.17 (m, 2H, –CH_2–CH$_3$), 4.37 (m, 4H, O–CH_2–CH_2–O). ^{31}P NMR (DMSO-d$_6$): δ 16.83.

2-Ethoxy-4-methyl-2-oxo-1,3,2-dioxaphospholane (5, EMEP)

5 was synthesized analogously to EEP to yield the desired product after distillation (34.5 g, 51%, b.p. 75–80 °C/0.1 Pa). ^{1}H NMR (CDCl$_3$): δ 1.37 (t, 3H, O–CH$_2$–CH_3, ^3J 6.0 Hz), 1.46 (q, 3H, –CH_3, ^3J 6.0 Hz), 3.91 (m, 1H, Me–CH–CH_2–O), 4.21 (m, 2H, O–CH_2–CH$_3$), 4.41 (m, 1H, Me–CH–CH_2–O), 4.75 (m, 1H, Me–CH–CH$_2$). ^{31}P NMR (DMSO-d$_6$): δ 15.65, 15.78.

General copolymerization procedure

The (co-)polymerization reactions were carried out in 25 mL Schlenk tubes. The tubes were flame-dried under vacuum, and purged with argon three times prior to use. In a typical copolymerization, EEP and EMEP were introduced into a tube with a syringe. Benzyl alcohol (55.9 mg; distilled and stored over molecular sieves 4 Å) was added to the mixture of EEP and EMEP with a syringe. TBD (22.7 mg) was dissolved in DCM (1.18 mL) and added to the mixture at 0 °C. After the solution had been stirred at 0 °C for 15 min, the copolymerization was terminated using a solution of acetic acid in DCM (20 mg mL^{-1}). The product was purified by repeated precipitation into cold diethyl ether. The desired copolymers were dried *in vacuo*. Yields: 74% to 95%.

Examples of representative NMR spectra

PEEP$_{32}$. ^{1}H NMR (DMSO-d$_6$): δ 7.40 (m, 5H, Ar), 5.04 (d, 2H, Ar–CH_2–O, ^3J 8.0 Hz), 4.88 (t, 0.8H, P–O–CH$_2$–CH$_2$–OH, ^3J 5.5 Hz), 4.22–4.13 (m, 124H, O–CH_2–CH_2–O), 4.12–4.03 (m, 64H, O–CH_2–CH$_3$), 3.96 (dt, 2H, P–O–CH_2–CH$_2$–OH, ^3J 7.2,

5.0 Hz), 3.57 (q, 2H, P–O–CH$_2$–CH_2–OH, ^3J 4.7 Hz), 1.26 (t, 96H, O–CH$_2$–CH_3, ^3J 7.0 Hz).
^{13}C NMR (DMSO-d$_6$): δ 128.43 (Ar), 128.38 (Ar), 127.82 (Ar), 68.85 (P–O–CH$_2$–CH$_2$–OH), 68.42 (Ar–CH$_2$–O), 66.07 (O–CH$_2$–CH$_2$–O), 63.74 (O–CH$_2$–CH$_3$), 60.03 (P–O–CH$_2$–CH$_2$–OH), 15.82 (O–CH$_2$–CH$_3$).
^{31}P NMR (DMSO-d$_6$): δ −0.97, −1.12, −1.23.

P(EEP$_{17}$-co-EMEP$_{16}$). ^{1}H NMR (DMSO-d$_6$): δ 7.40 (m, 5H, Ar), 5.03 (dd, 2H, Ar–CH_2–O), 4.88 (br s, 1H, P–O–CH$_2$–CH$_2$–OH), 4.57 (s, 16H, O–CHMe–CH$_2$–O), 4.16–3.85 (m, 160H, O–CH_2–CH_2–O and O–CHMe–CH_2–O), 3.78 (br s, 2H, P–O–CH_2–CHMe–OH), 3.57 (br s, 1H, P–O–CH$_2$–CHMe–OH), 1.25 (m, 147H, O–CH$_2$–CH_3 and O–CH(CH_3)–CH$_2$–O).
^{13}C NMR (DMSO-d$_6$): δ 128.48 (Ar), 127.81 (Ar), 73.33 (O-CHMe–CH$_2$–O), 69.28 (O–CHMe–CH$_2$–O), 66.07 (O–CH$_2$–CH$_2$–O), 63.74 and 63.57 (O–CH$_2$–CH$_3$), 17.15 (O–CH(CH$_3$)–CH$_2$–O), 15.85 and 15.80 (O–CH$_2$–CH$_3$).
^{31}P NMR (DMSO-d$_6$): δ −0.98, −1.12, −1.23, −1.28, −1.75, −1.89, −1.93, −1.95, −2.07, −2.13, −2.53, −3.02.

PEMEP$_{38}$. ^{1}H NMR (DMSO-d$_6$): δ 7.40 (m, 5H, Ar), 5.10–4.99 (m, 2H, Ar–CH_2–O), 4.58 (s, 38H, O–CHMe–CH$_2$–O), 4.25–3.88 (m, 150H, O–CHMe–CH_2–O), 3.84–3.74 (m, 2H, P–O–CH_2–CHMe–OH), 1.25 (m, 226H, O–CH$_2$–CH_3 and O–CH(CH_3)–CH$_2$–O).
^{13}C NMR (DMSO-d$_6$): δ 128.32 (Ar), 128.16 (Ar), 127.58 (Ar), 73.18 (O–CHMe–CH$_2$–O), 69.14 (O–CHMe–CH$_2$–O), 68.20 (Ar–CH$_2$–O), 63.46 (O–CH$_2$–CH$_3$), 17.07 (O–CH(CH$_3$)–CH$_2$–O), 15.70 (O–CH$_2$–CH$_3$).
^{31}P NMR (DMSO-d$_6$): δ −1.18, −1.22, −1.30, −1.34, −1.95, −2.15, −2.58, −3.09, −3.50.

Analytical methods and characterization

Size-exclusion chromatography (SEC). SEC measurements were performed in DMF (containing 0.25 g L^{-1} of lithium bromide as an additive) with an Agilent 1100 Series as an integrated instrument, including a PSS HEMA column ($10^6/10^5/10^4$ g mol^{-1}), a UV (275 nm), and a refractive index (RI) detector. Calibration was carried out using poly(ethylene glycol) standards provided by Polymer Standards Service.

Nuclear magnetic resonance (NMR) spectroscopy. The ^{1}H-, ^{13}C- and ^{31}P-NMR experiments were performed with a 5 mm BBFO z-gradient probe on the 500 MHz Bruker AVANCE III system. The temperature was kept at 298.3 K and calibrated with a standard ^{1}H methanol NMR sample using the topspin 3.0 software (Bruker). The ^{13}C NMR (125 MHz) and ^{31}P NMR (202 MHz) measurements were obtained with a ^{1}H powergate decoupling method using 30° degree flip angle, which had a 13 μs long 90° pulse for carbon and an 11 μs long 90° pulse for phosphorus. Additionally integratable ^{31}P experiments (inverse gated decoupling) were conducted with a relaxation delay of 10 s and 128 scans. For a ^{1}H NMR (500 MHz) spectrum 128 transients were used with a 10 μs long 90° pulse and a 12600 Hz spectral width together with a recycling delay of 5 s. Additionally carbon spectra were kept with a J-modulated spin-echo for ^{13}C-nuclei coupled to ^{1}H to determine the number of attached protons with decoupling during acquisition. The spectral

widths were 27 500 Hz (220 ppm) for ^{13}C and 30 000 Hz (150 ppm) for ^{31}P, both nuclei with a relaxation delay of 2 s. 2D (^1H, X (with X = ^{13}C and ^{31}P) HSQC and HMBC) were done on a Bruker Avance III 500 NMR spectrometer with a 5 mm BBFO probe equipped with a z-gradient. 2D ^1H–^{13}C-HMBC (heteronuclear multiple bond correlation via heteronuclear zero and double quantum coherence optimized on long range couplings with a low-pass J-filter to suppress one-bond correlations and no decoupling during acquisition using gradient pulses for selection). $^nJ_{CH}$ = 3 Hz for optimizing observable intensities of crosspeaks from multiple bond ^1H–^{13}C correlation. Similar experiments were done for 2D ^1H–^{31}P-HMBC with $^nJ_{PH}$ = 8 Hz. The spectra were referenced to the residual DMSO (^1H) = 2.50 ppm. All 1D spectra were processed with MestReNova 6.1.1-6384 software.

The DOSY (Diffusion Ordered Spectroscopy) experiments were executed with a 5 mm BBFO ^1H/X z-gradient probe and a gradient strength of 5.516 [G mm^{-1}] on the 500 MHz spectrometer. The gradient strength was calibrated using the diffusion coefficient of a sample of ^2H_2O/^1H_2O at a defined temperature and compared with the literature.[33,34] In this work, the gradient strength was 32 steps from 2% to 100%. The diffusion time d_{20} was optimised to 70 ms and the gradient length p_{30} was kept at 1.4 ms. All measurements were done with a relaxation delay of 1.5 s.

Turbidimetry measurements. Cloud points were determined in PBS pH 7.4 (10 mM) prepared from MilliQ water (18.2 mΩ) at a concentration of 10.0 mg mL^{-1} and observed by optical transmittance of a light beam (λ = 500 nm) through a 1 cm sample quartz cell. The measurements were performed with a Jasco V-630 photospectrometer with a Jasco ETC-717 Peltier element. The intensities of the transmitted light were recorded versus the temperature of the sample cell. The relative intensity of the transmitted light was calculated by division over the transmitted light of the pure solvent. The heating/cooling rate was 1 °C min^{-1} and values were recorded every 0.1 °C.

Differential scanning calorimetry. DSC measurements were performed using a Perkin-Elmer 7 series thermal analysis system and a Perkin Elmer Thermal Analysis Controller TAC 7/DX in the temperature range from −100 to 80 °C under nitrogen. The heating rate of 10 °C min^{-1} was employed.

Cytotoxicity test

The effect of phosphoester-co-polymers on the viability of a human cervical cancer cell line (HeLa) was measured with a commercial fluorescence assay PrestoBlue® (Life Technologies, Germany). The assay was based on the reduction of nonfluorescent resazurin into fluorescent resorufin by metabolic active cells.[35] HeLa cells were cultured in Dulbecco's modified eagle medium (DMEM), supplemented with 10% FCS, 100 units of penicillin and 100 mg mL^{-1} streptomycin, 2 × 10^{-3} M L-glutamine (all from Invitrogen, Germany). Cells were grown in a humidified incubator at 37 °C and 5% CO$_2$. For determining the cell viability, HeLa cells were seeded at a density of 15 000 cells cm^{-2} in 96-well plates (black, opaquewalled, Corning, Netherlands). Phosphoester-co-polymers were dissolved in sterile water (10 mg mL^{-1}, Ampuwa®, pH 7.4, Fresenius Kabi, Germany) and the indicated concentrations were produced by a serial dilution in cell culture medium (DMEM, 10% FCS). After 24 h, the culture medium was replaced by the phosphoester-co-polymer supplemented medium (200 µL, DMEM, 10% FCS) or the medium without compound (DMEM, 10% FCS) as a specific control for 100% cell viability. The cells were treated for 48 h and the number of viable cells was determined by the PrestoBlue® assay following the manufacturer's instructions. The fluorescence was detected with a plate reader (Infinite M1000, Tecan, Germany) at an excitation of 560 nm (±10 nm) and an emission of 590 nm (±10 nm) using i-control software (Tecan, Germany). The values represent the mean ± SD of 6 replicates and were plotted relative to the untreated cells.

Results and discussion

Monomer synthesis

The monomer 2-ethoxy-4-methyl-2-oxo-1,3,2-dioxaphospholane (EMEP, 5) was synthesized from racemic 1,2-propanediol and one equivalent of phosphorus trichloride to form 2-chloro-4-methyl-1,3,2-dioxaphospholane which was subsequently oxidized with oxygen in benzene at 50 °C. For safety reasons, a closed setup was used to pass oxygen through the solution continuously via a peristaltic pump (Fig. S1, ESI†). After distillation under reduced pressure, CMOP (4) was esterified with ethanol, according to the synthesis of EEP that has been reported previously.[36] EMEP was obtained by vacuum distillation and high purity was confirmed by ^1H and ^{31}P NMR spectroscopies. In contrast to EEP that shows a single phosphorus resonance at 16.83 ppm, EMEP exhibits two distinct signals in the ^{31}P NMR spectrum (Fig. S2, ESI†) corresponding to the two possible diastereomers arising from the racemic diol used for the synthesis and the asymmetric phosphorus (Scheme 2). The signals at 15.65 and 15.78 ppm also suggest the successful formation of a strained phosphate ring structure since strained dioxaphospholanes are known to exhibit a chemical shift to lower field in ^{31}P NMR compared to their corresponding open forms (PPEs usually show resonances at δ < 0.00 ppm). ^1H NMR spectra also confirmed the structure (compare the Experimental part and Fig. S3, ESI†).

Copolymerization of EEP and EMEP

Anionic ring-opening polymerization (AROP) allows the precise control of molecular weight and comonomer content of the resulting copolymers. Well-defined PPEs with narrow molecular weight distributions (MWD) were obtained previously with TBD as an organo-catalyst for homopolymerization of IPP.[16] TBD has furthermore proven to be especially effective in copolymerization of structurally different phospholane monomers as reported by Wooley and coworkers since TBD is a strong hydrogen bond acceptor (Scheme 3) making it a very active catalyst for the polymerization.[37] With TBD as the organocatalytic system both the activation of the nucleophile by acting as a hydrogen-bond acceptor and the activation of the monomer by formation of a
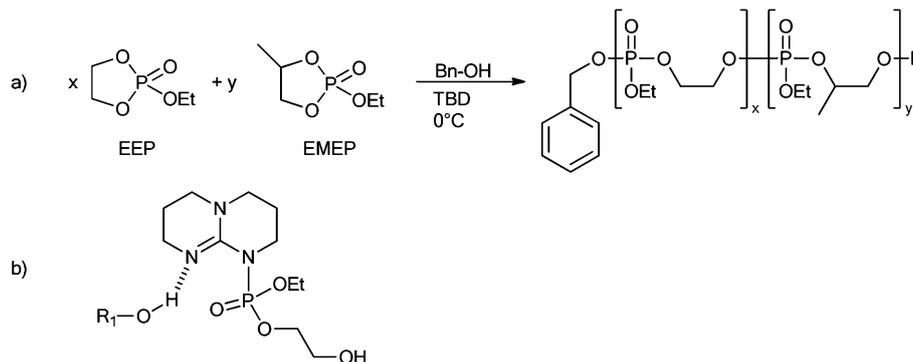
Scheme 3 (a) Copolymerization of EEP and EMEP. (b) Proposed mechanism of how TBD activates both the initiator or the propagating species (ROH) and the monomer.[36]

phosphoramidate (hydrogen-bond donor) are provided (compare Scheme 3).[36] As a result, TBD allows copolymerization of structurally different phosphate monomers reaching high conversion in only a few minutes but keeping polydispersity low.

Herein, we report the copolymerization of EEP and EMEP with TBD conducted at 0 °C in a sealed system for 15 min to reach full conversion. Benzyl alcohol was used as the initiator since the aromatic protons, as well as the methylene protons of the benzyl group, allow a calculation of the molecular weight from the ^1H NMR spectra (see Fig. S4, ESI†). All (co)polymerization reactions were terminated with an excess of acetic acid.

A series of copolymers with molecular weights of *ca.* 5000 g mol^{-1} and varying comonomer ratios was synthesized as summarized in Table 1. SEC chromatograms of all polymers showed a narrow molecular weight distribution (Fig. S5, ESI†) indicating the absence of transesterification reactions during the polymerization which could hamper the microstructure analysis. The degrees of polymerization expected from the monomer feeds agreed with those obtained from ^1H NMR end group analysis. The copolymer compositions were also calculated from the ^1H NMR spectra, based on a comparison of the integrals of the methanetriyl resonances of EMEP (at 4.58 ppm) and the

resonances of the methyl protons from both monomers from 1.30 to 1.25 ppm. As expected, all polymers exhibit low T_gs between *ca.* −50 °C corresponding to pure PEEP and *ca.* −40 °C for pure PEMEP. The T_gs for all copolymers are summarized in Table 1. A gradual increase in T_g with increasing EMEP can be observed (Fig. S6, ESI†) indicating a random monomer incorporation.

Detailed microstructure investigation of all copolymers has been performed employing ^1H NMR, ^{31}P NMR, $^1H^{31}P$ HMBC NMR, ^{13}C NMR and $^1H^{13}C$ HMBC NMR spectroscopies. In the ^{31}P NMR spectra a signal pattern can be detected that has similarly been reported by Penczek and coworkers for the corresponding poly-*H*-phosphonate.[28] The analysis of the pattern reveals all possible dyads resulting from α- and β-ring-opening, which are shown in Scheme 4.

Obviously, αα and ββ ring-openings lead to the same dyads (*i.e.* head–tail, HT) and therefore to the same chemical environment for the phosphate group, however αβ and βα ring-openings lead to tail-to-tail (TT) and head-to-head (HH) dyads, respectively.

If racemic EMEP is polymerized, these dyads have three centers of chirality, namely the adjacent methylene or methanetriyl group, the ester and the phosphorus atom. The

Table 1 Synthetic results of P(EEP-*co*-EMEP)

Code[a]	[EEP]$_0$/[EMEP]$_0$	Yield[b] (%)	$M_{n(theo)}$[c]/g mol^{-1}	DP[a]	M_n[a]/g mol^{-1}	M_n[d]/g mol^{-1}	M_w[d]/g mol^{-1}	M_w/M_n[d]	T_g/°C
PEEP$_{32}$	100 : 0	99	5100	32	5000	2500	3300	1.32	−47
P(EEP$_{31}$-*co*-EMEP$_2$)	90 : 10	95	5100	33	5100	2500	3000	1.19	−47
P(EEP$_{28}$-*co*-EMEP$_5$)	80 : 20	94	5100	33	5100	2800	3400	1.25	−49
P(EEP$_{31}$-*co*-EMEP$_7$)	70 : 30	94	5100	38	5900	2300	3000	1.29	−46
P(EEP$_{22}$-*co*-EMEP$_{11}$)	60 : 40	93	5100	33	5200	2200	2800	1.28	−44
P(EEP$_{17}$-*co*-EMEP$_{13}$)	50 : 50	91	5100	30	4800	2100	2600	1.25	−44
P(EEP$_{17}$-*co*-EMEP$_{16}$)	40 : 60	89	5100	33	5200	2100	2700	1.32	−43
P(EEP$_{13}$-*co*-EMEP$_{20}$)	30 : 70	86	5100	33	5300	2100	2500	1.22	−42
P(EEP$_8$-*co*-EMEP$_{25}$)	20 : 80	74	5200	33	5400	2000	2400	1.22	−40
P(EEP$_4$-*co*-EMEP$_{29}$)	10 : 90	77	5200	33	5400	1900	2300	1.20	−42
PEMEP$_{16}$	0 : 100	75	2200	16	2800	1800	2200	1.22	−39
PEMEP$_{38}$	0 : 100	73	5800	38	6400	2300	3600	1.56	−37
PEMEP$_{52}$	0 : 100	49	8700	52	8800	2700	4000	1.47	−40

[a] Degree of polymerization (DP) of the (co)monomers and the number average of molecular weight (M_n) were determined by ^1H NMR. [b] Determined by weight. [c] Theoretical molecular weight calculated from the monomer : initiator ratio. [d] Determined by SEC in DMF at 50 °C *vs.* PEG standards.
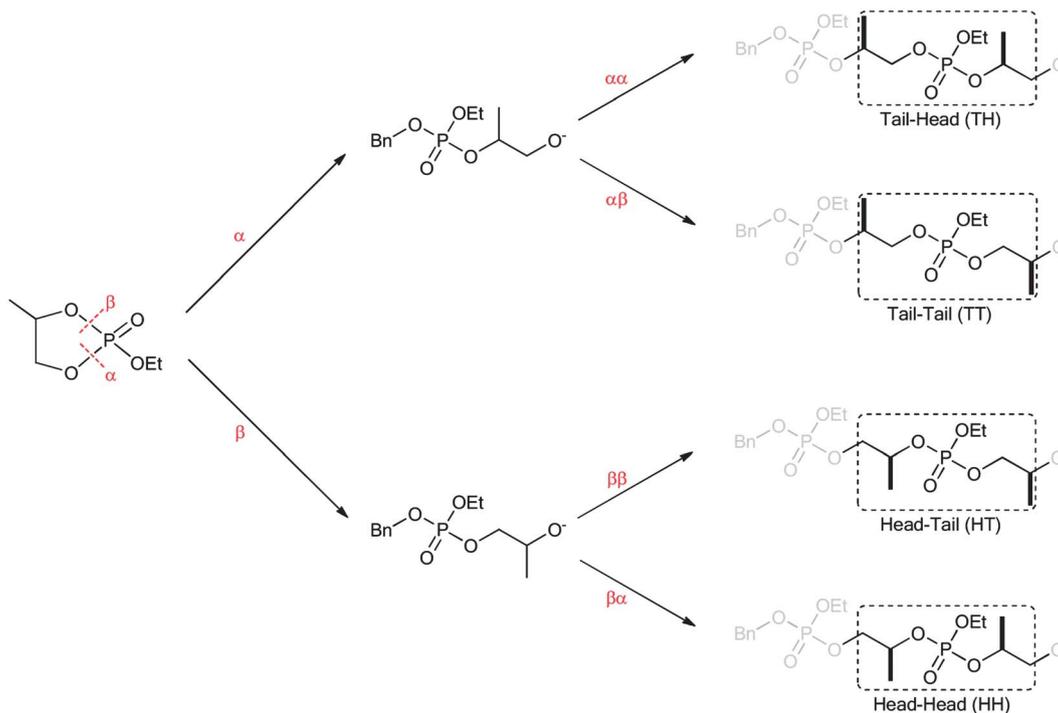
**Scheme 4** Possible dyads arising from α- and β-ring-openings (the methyl group was highlighted).

homopolymer derived from EMEP can therefore contain eight head-to-tail structures resulting from αα or ββ ring-openings (Fig. 1). These environments (and thus chemical shifts) are found with the increasing intensity in copolymers with EEP with the increasing EMEP content.

The structures within the dashed boxes are enantiomers and therefore magnetically equivalent while the other combinations result in diastereomers. ^{31}P NMR can only distinguish between these four different structures arising from head-to-tail structures. The same analysis can be done for the head-to-head (βα) and the tail-to-tail dyads (αβ) (compare Fig. S7, ESI†).

This microstructure analysis leads to 10 distinct signals in the high resolution ^{31}P NMR spectra (202 MHz). Penczek and coworkers have acquired a similar dyad model for the studied poly-H-phosphonates, but were unable to observe all expected

signals experimentally due to a limited NMR setup with 36.43 MHz for the phosphorus resonance.[28] They approximated that the chemical shift of the phosphorus atoms is only affected by the nearest environment which reduces the possible (magnetically not equivalent) dyad structures to six units. The same approximation can be applied for PEMEP (Fig. 2).

Detailed structural investigations by NMR of all polymers synthesized in this study and the assignment of the resonances rely on the analysis of the homopolymers, PEEP and PEMEP. The backbone of PEEP bears no chiral center besides the phosphorus and is therefore a model compound for the tail-to-tail structure of PEMEP and its copolymers with EEP. The ^{31}P NMR spectrum reveals three distinct signals, which can be attributed to the starting unit (phosphate next to the initiating benzyl group) at $\delta = -1.12$ ppm, the backbone representing a
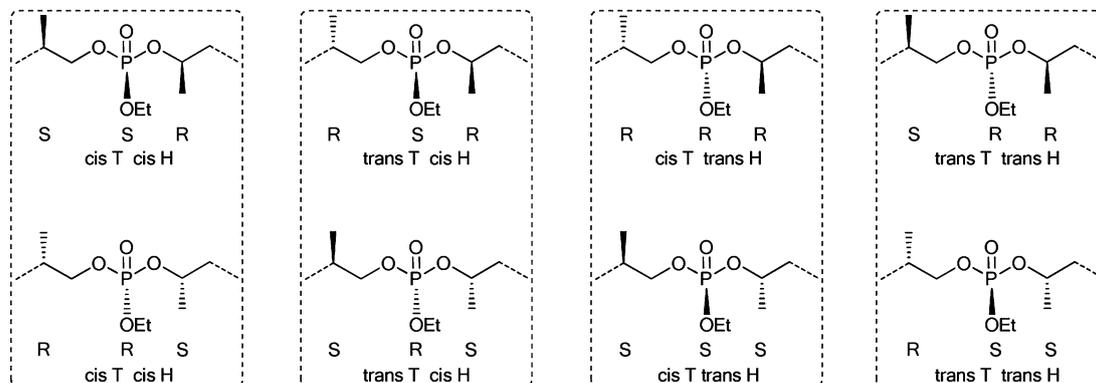
Fig. 1 Dyad analysis of all possible tail-to-head (TH) configurations of PEMEP.
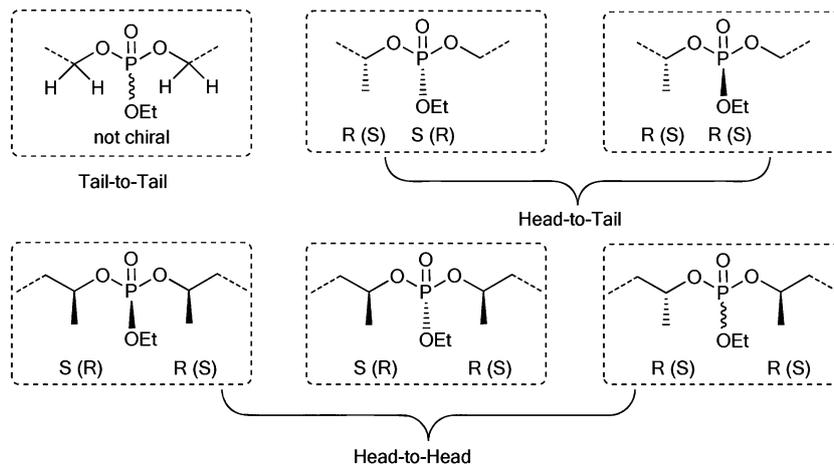
Fig. 2 Six possible dyads of P(EEP-*co*-EMEP) that are magnetically not equivalent (structures within dashed boxes are enantiomers and chemically equivalent).

variety of different chemical environments leading to a broad and predominant signal at $\delta = -1.23$ ppm, and the terminal unit at $\delta = -0.97$ ppm (Fig. 3, vertical axis). This assignment was proven by $^1H^{31}P$ HMBC NMR spectroscopy indicating coupling between the methylene protons of the benzyl initiator (H^I) and the phosphorus (P^I) of the first monomer unit at $\delta_P = -1.12$. Furthermore, strong coupling of the backbone phosphate groups (P^B) and the adjacent ethylene glycol (H^{EG}) and ethoxy-groups (H^{O-CH_2-Me}) is obvious. The terminal phosphorus center (P^T) at $\delta_P = -0.97$ does not show coupling with the terminal hydroxyl functionality at $\delta_H = 4.88$ (Fig. 3).

In the high resolution ^{31}P NMR spectra of all other (co) polymers, three different regions can be defined (Fig. 4): the

first region at the lowest field between *ca.* -1.00 and -1.50 ppm houses signals arising from tail-to-tail structures (the only signal for PEEP plus two small signals stemming from the first and the last phosphate unit along the polymer chain, Fig. 4, top). The second region at a higher field from -1.50 to -2.30 ppm contains signals from the head-to-tail adducts which are the dominant signals of this spectrum because of the highest probability of formation. These resonances show strong coupling to the adjacent methyl-group of EMEP in $^1H^{31}P$ NMR. Therefore head-to-tail microstructures as shown in Fig. 2 can be assigned to these resonances.

At higher field, from -2.30 to -3.50 ppm, the head-to-head structures show three distinct signals. The resonance at
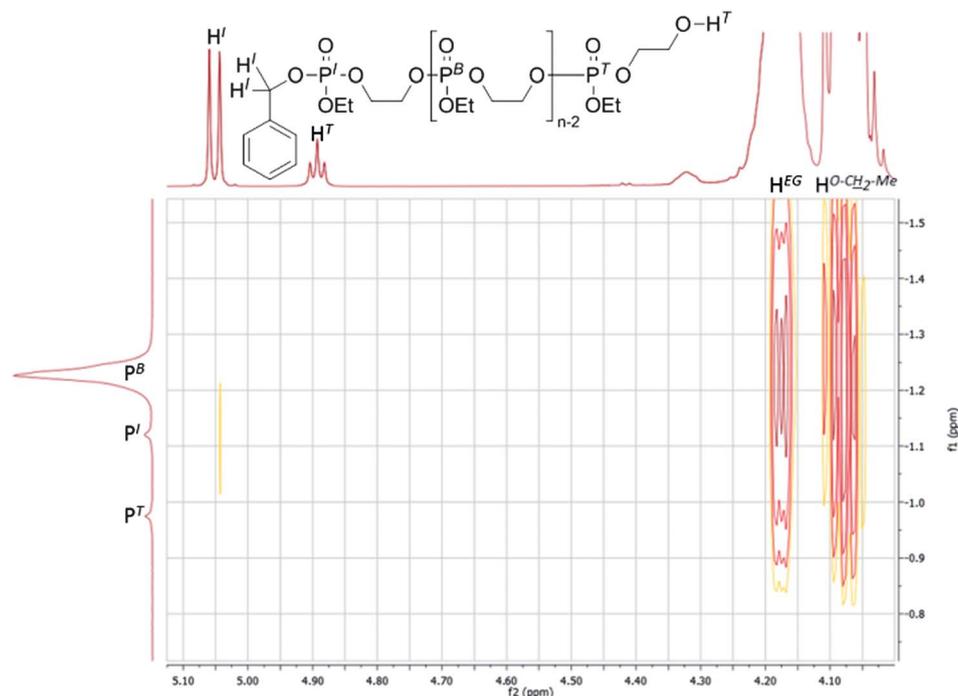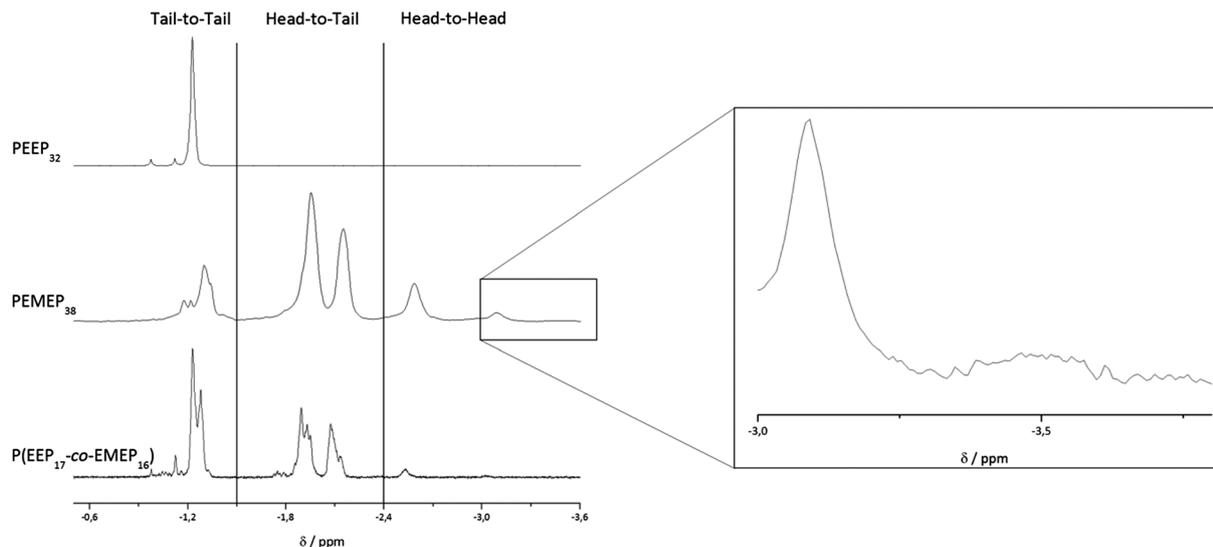

Fig. 3 $^1H^{31}P$ HMBC NMR of PEEP$_{32}$ in DMSO-d$_6$. Cross-coupling between the different phosphorus species and protons is revealed.

Fig. 4 ^{31}P NMR (202 MHz) spectra of PEEP$_{32}$ (top), PEMEP$_{38}$ (middle) and P(EEP$_{17}$-co-EMEP$_{16}$) (bottom) in DMSO-d$_6$. Three distinct regions can be defined in the spectrum corresponding to the three different dyad structures.

−2.58 ppm gives a stronger signal compared to the resonance at $\delta = -3.09$ ppm and the weak signal at $\delta = -3.50$ ppm. This decrease in intensity, when shifting to higher field, is attributed to a decline in probability of formation indicating structures that become more and more unlikely to form. The inset in the middle spectrum of PEMEP$_{38}$ shows a resonance at −3.50 ppm corresponding to the head-to-head structure which is formed least (region magnified). Detailed theoretical microstructure analysis and application of the developed dyad model allowed the assignment of the signals in high resolution ^{31}P NMR spectra. Focusing on the tail-to-tail region (Fig. 4), it becomes obvious that the backbone signal of PEEP ($\delta = -1.24$ ppm) decreases with the increasing EMEP content, while subsequently two other signals, at −1.28 and −1.33 ppm, start to increase (Fig. S8, ESI†). Both the new signals can therefore be attributed to the two possible microstructures in which the phosphate is adjacent to two methylene groups (Fig. S9, ESI†). This observation is conclusively substantiated by ^{1}H^{31}P NMR spectroscopy lacking coupling between the phosphate and the methyl groups of EMEP (Fig. S10, ESI†). In the copolymers, the dominating signal at −1.28 ppm is attributed to the sequence EEP–EMEP$_{\alpha}$ (the subscript indicates that EMEP was ring-opened in an α-fashion). Consequently, the only remaining resonance at −1.33 ppm can be attributed to the EMEP$_{\alpha}$–EMEP$_{\beta}$ dyad (Fig. S8, ESI†). The formation of this microstructure is quite unlikely, since the AROP of EMEP gives predominantly, but not exclusively, the α-ring-opened products.

The head-to-head region in the ^{31}P NMR spectra of the copolymers contains three signals at −2.53 ppm, −3.09 ppm and −3.50 ppm, whereas the latter is only observed for the homopolymer, PEMEP. The developed dyad model allows the estimation that the dominant signal of this region, at −2.53 ppm, corresponds to the only microstructure of the three possible options which is not a meso-compound. This assumption relies on the fact that this microstructure is the

most probable one – of the three – to occur. The other two signals can be assigned to the sterically less hindered ($\delta = -3.09$ ppm) and the sterically most demanding microstructure ($\delta = -3.50$ ppm), the latter most improbable of formation and therefore only observed for PEMEP.

Copolymers of EEP and EMEP show with the increasing amount of EMEP, increasing signals for the head-to-tail and the head-to-head region, because of the introduction of phosphate centers with an asymmetrical substitution pattern.

The random incorporation of the respective phospholane comonomers in the polyphosphate backbone is of great interest for its potential bioapplications due to the possible aggregation and different hydrolytic degradation kinetics. A strong indication for a random copolymerization can be derived from the ^{1}H^{31}P HMBC NMR spectra as the resonance of the methylene protons of the initiating benzyl alcohol ($\delta = 5.05$ ppm) show coupling both to phosphorus in the tail-to-tail region and also in the head-to-tail region (Fig. S10, ESI†). In contrast, for the homo-PEMEP this methylene group only couples to phosphorus of the head-to-tail region indicating that the first monomer is opened in an α-fashion – this also supports the assumption that α-ring-opening is preferred over β-ring-opening. Also in the ^{1}H NMR spectra of the copolymers the signals of the methylene protons (H^{I}) of the initiating benzyl group can be used as a sensor for monomer incorporation; in the homopolymer PEEP they result in a doublet due to coupling to phosphorus (^{3}J coupling, Fig. 3 or 5, bottom). The ^{1}H NMR spectra of the copolymers, however, show an increasing second pair of methylene signals arising with the increasing EMEP content at a slightly higher field (Fig. 5). At the same time, the signals at $\delta = 5.05$ ppm decrease with the decreasing EEP content. Also the resonance of the terminal OH group (H^{T} at 4.89 ppm) indicates the occurrence of different chain ends due to primary or secondary OH groups as the signal becomes broader in the copolymers. The increasing EMEP content can be determined

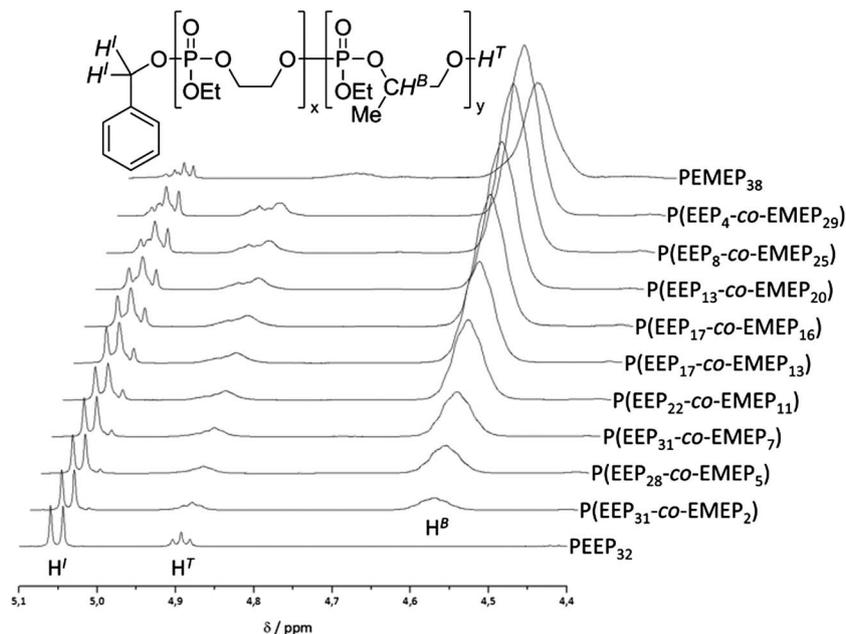**Fig. 5** Comparison of ^{1}H NMR spectra of different P(EEP-co-EMEP) copolymers measured in DMSO-d$_6$.

by the resonance of the methanetriyl proton at 4.58 ppm (H^B). A similar strategy was used by Lynd and coworkers to determine copolymerization parameters for the copolymerization of ethylene oxide with allyl glycidyl ether or ethylene glycol vinyl glycidyl ether by monitoring the signal splitting of the initiator signals in ^{1}H NMR.[38] Furthermore, the thermal properties were derived from DSC (compare Table 1 and Fig. S6†), *i.e.* the gradual increase of the glass transition temperature from pure PEEP (−47 °C) with the increasing EMEP content to the expected value of the PEMEP homopolymer (−39 °C).

Furthermore, all copolymers were investigated *via* ^{1}H diffusion ordered spectroscopy (DOSY) to verify that all signals of both comonomers and the initiators that are visible in the ^{1}H NMR spectrum belong to polymer chains with similar diffusion coefficients in the range of 5–9 × 10^{-7} m^2 s^{-1} in DMSO-d$_6$ (Fig. S11, ESI†). This observation can also be attributed to the successful copolymerization, incorporating all monomer units without formation of two homopolymers (which should show two different diffusion coefficients, especially for copolymers with very different feed ratios).

In vitro cytotoxicity

Biocompatibility is an important issue when developing new polymers for biomedical applications. Most nonionic PPEs, such as PEEP, that have been reported to date are nontoxic polymers.[39] The herein presented PEMEP and the respective copolymers with EEP were expected to be nontoxic and the degradation products are harmless compounds, namely phosphate and propanediol, which prevent any polymer accumulation in the body. The cytotoxicity of the P(EEP-co-EMEP) copolymers was investigated *in vitro* against a human cervical cancer cell line (HeLa) in a concentration range of 1–600 μg mL^{-1} by measuring the
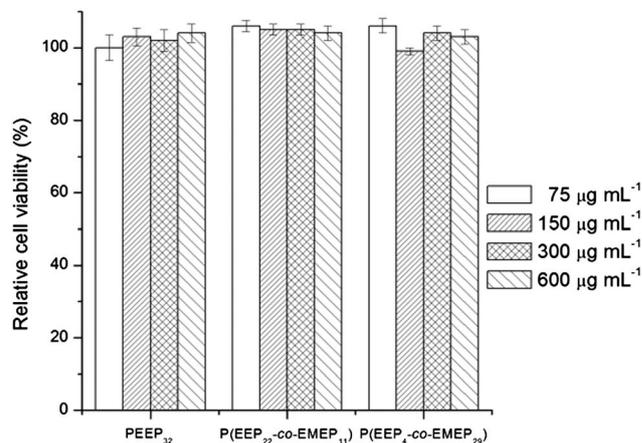

Fig. 6 *In vitro* cell viability of HeLa cells treated with PEEP$_{32}$, P(EEP$_{22}$-co-EMEP$_{11}$) and P(EEP$_4$-co-EMEP$_{29}$) after 48 h of incubation. Untreated cells were set to 100%. The experiments were carried out as 6 independent replicates and repeated twice.

metabolic activity as the ATP content of viable cells in relation to untreated cells. The results are displayed in Fig. 6 and prove a very good biocompatibility for the novel copolymers, comparable to PEEP. No adverse effects on the viability were observed, indicating good biocompatibility of the synthesized copolymers comparable to PEEP.

Thermoresponsive behavior

Thermoresponsive polymers are of great interest in biomedical research with possible applications in smart drug/gene delivery systems and tissue engineering. In particular the polymers derived from *N*-substituted acrylamides, such as

polyacrylamides[40–44] or PEG derivatives,[45,46] were found to undergo a reversible phase separation upon heating in an aqueous solution, exhibiting a LCST. Copolymerization is a typical tool to adjust the cloud point close to physiological relevant temperatures.

The cloud point temperature was determined for PEMEP with varying degrees of polymerization (from 16 to 42), and was found to be in the range of 23–27 °C (Fig. S12, ESI†) proving a higher water-solubility than the very similar PIPP that is insoluble in water at these temperatures. This proves our assumption that the introduction of a methyl group in the bridging element of PPEs has a lower influence on hydrophobicity than that in the side chain (as in the case of IPP). The cloud point temperatures increase when EEP as a comonomer is introduced (Fig. S13, ESI†). Interestingly, the molar ratio of EEP in the copolymer has only little influence on the cloud point temperature and all copolymers become insoluble in water at ca. 40–45 °C in water (at a concentration of 10 mg mL^{-1} in PBS pH 7.4 10 mM). We assume that this drastic shift of the cloud point is due to aggregation of PEMEP and also of the copolymers which is supported by dynamic light scattering and is currently under deeper investigation.

Conclusion

In this work, the successful copolymerization of 2-ethoxy-2-oxo-1,3,2-dioxaphospholane (EEP) and 2-ethoxy-4-methyl-2-oxo-1,3,2-dioxaphospholane (EMEP) through anionic ring-opening polymerization catalyzed by TBD was demonstrated for the first time. The synthesized copolymers with controlled molecular weights and narrow molecular weight distributions were investigated via NMR spectroscopy and random monomer incorporation is highly probable from detailed ^{1}H^{31}P HMBC NMR spectra revealing that both monomers are ring-opened to the same extent by the initiator. DSC measurements provided further evidence that no block or gradient-like structure has formed as the glass transition temperatures shift gradually from the value for PEMEP with the increasing amount of EEP to the pure PEEP. Furthermore, from the high resolution ^{31}P NMR spectra, 6 major resonances arise stemming from different dyads in the backbone. The signals were grouped in 3 different spectral regions depending on the possible dyad motifs: tail–tail (T–T), head–tail (H–T) and head–head (H–H). For copolymers with high EEP content, the T–T signal was dominant, since EMEP is mainly, but not exclusively, ring-opened in an α-fashion due to the steric demand of the additional methyl-group adjacent to the phosphate group of the monomer. Therefore, signals assigned to the H–T structures become dominant with the increasing EMEP content. The sterically demanding H–H motifs are also found in the spectra, especially for very high EMEP : EEP ratios, reinforcing that β-ring-opening is disfavored.

The obtained copolymers exhibited thermoresponsive behavior. A lower critical solution temperature (LCST) was observed for all copolymers. The LCSTs of aqueous P(EEP-co-EMEP) solutions showed only a small dependency on the copolymer composition. Only PEMEP exhibited a considerable shift to a lower LCST due to its higher degree of hydrophobicity. Investigation of underlying supramolecular structures explaining this unexpected behavior is under way.

Initial studies on the biocompatibility of the polyphosphates were carried out by treating HeLa cells with various concentrations of an aqueous solution of selected copolymers and excellent cell viability was observed. Such thermoresponsive P(EEP-co-EMEP)s are promising candidates for biomedical applications, e.g. for tissue engineering and controlled drug release systems, which is currently under investigation.

Acknowledgements

References

1 Y.-C. Wang, Y.-Y. Yuan, J.-Z. Du, X.-Z. Yang and J. Wang, *Macromol. Biosci.*, 2009, **9**, 1154–1164.

2 S.-W. Huang, J. Wang, P.-C. Zhang, H.-Q. Mao, R.-X. Zhuo and K. W. Leong, *Biomacromolecules*, 2004, **5**, 306–311.

3 M. Richards, B. I. Dahiyat, D. M. Arm, P. R. Brown and K. W. Leong, *J. Biomed. Mater. Res.*, 1991, **25**, 1151–1167.

4 C. Wachiralarpphaithoon, Y. Iwasaki and K. Akiyoshi, *Biomaterials*, 2007, **28**, 984–993.

5 J. Baran, P. Klosinski and S. Penczek, *Makromol. Chem.*, 1989, **190**, 1903–1917.

6 J. Pretula and S. Penczek, *Makromol. Chem.*, 1990, **191**, 671–680.

7 S. Penczek, A. Duda, K. Kałużynski, G. Lapienis, A. Nyk and R. Szymanski, *Makromol. Chem., Macromol. Symp.*, 1993, **73**, 91–101.

8 S. Penczek, G. Lapienis, K. Kałużynski and A. Nyk, *Pol. J. Chem.*, 1994, **68**, 2129–2142.

9 K. Kałużynski, J. Libisowski and S. Penczek, *Macromolecules*, 1976, **9**, 365–367.

10 P. Klosinski and S. Penczek, *Macromolecules*, 1983, **16**, 316–320.

11 J. Libiszowski, K. Kałużynski and S. Penczek, *J. Polym. Sci., Polym. Chem. Ed.*, 1978, **16**, 1275–1283.

12 T. Steinbach, E. Alexandrino and F. R. Wurm, *Polym. Chem.*, 2013, **4**, 3800–3806.

13 F. Marsico, M. Wagner, K. Landfester and F. R. Wurm, *Macromolecules*, 2012, **45**, 8511–8518.

14 C.-S. Xiao, Y.-C. Wang, J.-Z. Du, X.-S. Chen and J. Wang, *Macromolecules*, 2006, **39**, 6825–6831.

15 D.-P. Chen and J. Wang, *Macromolecules*, 2005, **39**, 473–475.

16 Y. Iwasaki and E. Yamaguchi, *Macromolecules*, 2010, **43**, 2664–2666.

17 Y. Iwasaki, C. Wachiralarpphaithoon and K. Akiyoshi, *Macromolecules*, 2007, **40**, 8136–8138.

18 Y. G. Takei, T. Aoki, K. Sanui, N. Ogata, T. Okano and Y. Sakurai, *Bioconjugate Chem.*, 1993, **4**, 341–346.

19 Y. Tachibana, M. Kurisawa, H. Uyama, T. Kakuchi and S. Kobayashi, *Chem. Commun.*, 2003, 106–107.

20 C. Mangold, B. Obermeier, F. Wurm and H. Frey, *Macromol. Rapid Commun.*, 2011, **32**, 1930–1934.

21 C. Tonhauser, A. Alkan, M. Schömer, C. Dingels, S. Ritz, V. Mailänder, H. Frey and F. R. Wurm, *Macromolecules*, 2013, **46**, 647–655.

22 J. A. Ruddick, *Toxicol. Appl. Pharmacol.*, 1972, **21**, 102–111.

23 O. N. Miller and G. Bazzano, *Ann. N. Y. Acad. Sci.*, 1965, **119**, 957–973.

24 A. Zwierzak, *Can. J. Chem.*, 1967, **45**(21), 2501–2512.

25 J. S. N. E. E. Nifant'ev and A. A. Borisenko, *J. Gen. Chem. USSR (Engl. Transl.)*, 1971, **41**, 1885.

26 S. Penczek, J. Pretula and K. Kaluzynski, *Biomacromolecules*, 2005, **6**, 547–551.

27 T. Biela, S. Penczek, S. Slomkowski and O. Vogl, *Makromol. Chem. Rapid Commun.*, 1982, **3**, 667–671.

28 T. Biela, P. Kłosiński and S. Penczek, *J. Polym. Sci., Part A: Polym. Chem.*, 1989, **27**, 763–774.

29 L. Fontaine, D. Derouet and J. C. Brosse, *Eur. Polym. J.*, 1990, **26**, 865–870.

30 L. Fontaine, D. Derouet and J. C. Brosse, *Eur. Polym. J.*, 1990, **26**, 857–863.

31 R. S. Edmundson, *Chem. Ind. (London, U. K.)*, 1962, 1828–1829.

32 H. J. Lucas, F. W. Mitchell and C. N. Scully, *J. Am. Chem. Soc.*, 1950, **72**, 5491–5497.

33 A. Jerschow and N. Müller, *J. Magn. Reson., Ser. A*, 1996, **123**, 222–225.

34 A. Jerschow and N. Müller, *J. Magn. Reson.*, 1997, **125**, 372–375.

35 S. N. Rampersad, *Sensors*, 2012, **12**, 12347–12360.

36 C. Benoît, G. Bruno, K. Leo, J. Christine and L. Philippe, *Macromolecules*, 2012, **45**, 4476–4486.

37 S. Zhang, A. Li, J. Zou, L. Y. Lin and K. L. Wooley, *ACS Macro Lett.*, 2012, **1**, 328–333.

38 B. Lee, M. Wolffs, K. Delaney, J. Sprafke, F. Leibfarth, C. Hawker and N. Lynd, *Macromolecules*, 2012, **45**, 3722–3731.

39 Y.-C. Wang, L.-Y. Tang, T.-M. Sun, C.-H. Li, M.-H. Xiong and J. Wang, *Biomacromolecules*, 2008, **9**, 388–395.

40 F. M. Winnik, H. Ringsdorf and J. Venzmer, *Langmuir*, 1991, **7**, 905–911.

41 F. M. Winnik, H. Ringsdorf and J. Venzmer, *Langmuir*, 1991, **7**, 912–917.

42 H. G. Schild and D. A. Tirrell, *J. Phys. Chem.*, 1990, **94**, 4352–4356.

43 H. G. Schild, *Prog. Polym. Sci.*, 1992, **17**, 163–249.

44 L. D. Taylor and L. D. Cerankowski, *J. Polym. Sci., Polym. Chem. Ed.*, 1975, **13**, 2551–2570.

45 J.-F. Lutz, *Adv. Mater.*, 2011, **23**, 2237–2243.

46 C. Mangold, F. Wurm and H. Frey, *Polym. Chem.*, 2012, **3**, 1714–1721.